Journal of Structural Geology, Vol. 3, No. 2, pp. 109 to 116, 1981
Printed in Great Britain

0191-8141/81/020109-08 $02.00/0

Analysis of three-dimensional strain modified uniform distributions: andalusite fabrics from a granite aureole

DAVID J. SANDERSON and ALAN W. MENEILLY

Department of Geology, The Queen's University of Belfast,
Belfast BT7 1NN, Northern Ireland

(*Received* 21 *July* 1980; *accepted in revised form* 7 *January* 1981)

Abstract — A method of analysing finite strain from an initial random distribution of lines or planes is presented. The shape of the strain ellipsoid is mapped to the eigenvalue ratios of an orientation matrix. The method is used to interpret the andalusite fabrics from the aureole of the Ardara granite, County Donegal, Ireland. The high flattening strains determined in the aureole are accompanied by oblate strains in the granite margins and support the concept of deformation produced by expansion of the pluton.

INTRODUCTION

STRAIN in general produces a change in length (extension) and change in orientation (rotation) of linear elements within a material. Much use has been made of these extensions and rotations with respect to objects of specific initial shape in the analysis of finite strain in rocks (Ramsay 1967).

Analysis of finite strain based on angular distributions of lines and planes has received little attention. Some progress has been made in relating deformed distributions of lines in two dimensions to strain ratios (Sanderson 1977). However, despite the development of the theory of strained angular density distributions by March (1932) and Owens (1973), little practical application in three dimensions has been attempted. In this paper we will outline a simple method for specifying angular distributions and show how this can be used to analyse distributions resulting from the deformation of uniform initial distributions.

DEFORMATION OF LINES AND PLANES

Owens (1973), developing the work of March (1932), gives a comprehensive treatment of the modification of angular density distributions of lines and planes by homogeneous strain. His treatment will be followed in outline here.

A line defined by a unit vector, $\mathbf{v}$, is transformed under a strain, S (where S is the deformation gradient tensor, Malvern 1969), to a vector $\mathbf{v}'$, which is generally not a unit vector, by:

$$\mathbf{v}' = \mathbf{S}\mathbf{v}. \tag{1}$$

Owens (1973) shows that the angular density, f', in a direction parallel to $\mathbf{v}'$ is related to the initial density, f, parallel to v, by:

$$f' = \lambda^{3/2} |\mathbf{S}|^{-1} f \tag{2}$$

where $|\mathbf{S}|$ is the determinant of S and λ is the quadratic elongation of the line.

Similarly a pole to a plane, $\mathbf{p}$, is transformed to $\mathbf{p}'$ by:

$$\mathbf{p}' = (\mathbf{S}^{-1})^T \mathbf{p} \tag{3}$$

and:

$$f' = \lambda'^{3/2} |\mathbf{S}| f \tag{4}$$

where λ' is the reciprocal quadratic elongation.

From these relationships the strain modified frequency distribution can be determined in terms of the initial distribution and the finite strain. In the general case the shape and orientation of the initial distribution and the deformation gradient tensor must be known relative to some reference frame.

The situation simplifies considerably if the initial distribution is uniform because the angular frequency, f, is constant and S may be factored into a stretch tensor, U, and a rotation tensor, R.

$$\mathbf{S} = \mathbf{UR}. \tag{5}$$

The operation of the rotation R on the uniform distribution leaves f unchanged. Thus equation (2) simplifies to:

$$f' = C_1 \lambda^{3/2}. \tag{6}$$

Similarly, for planes, equation (4) simplifies to:

$$f' = C_2 \lambda'^{3/2} \tag{7}$$

where $|\mathbf{S}|^{-1}$ is included with the constants because this term, which specifies the volume change during deformation, cannot be analysed from angular frequency distributions (Owens 1973).

Unbiased sampling of the strain modified uniform distribution allows the principal stretches to be calculated to a constant factor (C) and hence the strain ratios can be found. Since the strain modified uniform distribution was first studied by March (1932) we will term this distribution, in 3-dimensions, the March distribution.

The March distribution for either lines or planes has an orthorhombic or higher symmetry consisting of a bipolar maximum or a planar girdle (great circle) or, more generally, both. This follows directly from equations (6)

and (7) since λ and λ' have orthorhombic or higher symmetry.

SPECIFICATION OF FABRIC DATA

Orientation data obtained by sampling a density distribution may be plotted on an equal-area stereogram. The resulting fabric could then be compared with some distribution model, such as the March distribution, and an attempt made to estimate the parameters of the distribution ($\lambda_1 \geq \lambda_2 \geq \lambda_3$ for the March model). How is such an analysis best achieved?

One approach would be to estimate the angular density, f', in a number of directions. This is usually done by contouring the fabric diagram and large quantities of data are necessary to achieve reliable estimates.

The method of contouring will usually introduce bias errors in the estimation of the density at a point; all common contouring methods (e.g. Mellis, Schmidt etc.) introduce biased grouping errors.

Ramsden & Cruden (1979) have discussed this problem with respect to correcting estimates of maximum density in axially symmetric clustered data using the Fisher distribution model. This work may be applied to some March distributions with axial symmetry. This approach, however, has not yet been extended to orthorhombic distributions although such a treatment based on the Bingham distribution model should be possible.

Where data are numerous, direct estimation of strain from maximum, minimum and intermediate densities is possible. This method has been followed by Oertel (1970) and others to compare fabrics obtained from X-ray texture goniometry with the March model.

A convenient way to specify orthorhombic distributions is by an orientation tensor developed by Bingham (1964), Scheidegger (1964), Fara & Scheidegger (1963) and Watson (1965). The orientation tensor, **E**, is formed by summation of the cross-products of unit vectors, $\mathbf{v}_i$, (l_i, m_i, n_i) where l, m, and n are direction cosines.

$$\mathbf{E} = \frac{1}{n}\sum_{i=n}^{n} (\mathbf{v}_i^T \mathbf{v}_i)$$

$$= \frac{1}{n}\begin{bmatrix} \Sigma l_i^2 & \Sigma l_i m_i & \Sigma l_i n_i \\ \Sigma l_i m_i & \Sigma m_i^2 & \Sigma m_i n_i \\ \Sigma l_i n_i & \Sigma m_i n_i & \Sigma n_i^2 \end{bmatrix}. \quad (8)$$

If a direction is specified by $\mathbf{v}_i$ or its antipolar vector $\bar{\mathbf{v}}_i$ $(-l_i, -m_i, -n_i)$ then

$$\bar{\mathbf{v}}_i^T \bar{\mathbf{v}}_i = \mathbf{v}_i^T \mathbf{v}_i.$$

Therefore **E** depends only on the direction and not the sense of direction of the unit vector and can be used to specify axial data uniquely. Conversely the use of **E** to represent true vectors destroys information. The eigenvalues (E_1, E_2, E_3) and eigenvectors ($\mathbf{e}_1$, $\mathbf{e}_2$, $\mathbf{e}_3$) of **E** may be interpreted as measures of the shape and symmetry axes of the distribution provided it has orthorhombic or higher symmetry. For distributions with lower symmetry neither eigenvalues nor eigenvectors have a simple interpretation (cf. Woodcock 1977).

Most of the use and interpretation of **E** has been for orthorhombic distributions displaying a simple combination of bipolar maxima and/or planar girdles (e.g. Bingham 1964, Scheidegger 1964, Woodcock 1977). A common misconception, although not attributable to the authors above, is that the orientation tensor specifies a distribution of unique shape. This is not true even if the orthorhombic distribution consists of simple bipolar maxima and/or girdles. For example, the March and Bingham distributions are two such distributions whose angular densities are different for distributions with the same orientation tensor, **E**.

In order to relate distribution parameters (e.g. κ_j in the Bingham distribution or λ_j in the March distribution) to the eigenvalues we must assume or, better still, establish a close correspondence between the angular densities for the sample and the distribution model. Many distributions have a unique correspondence between eigenvalues of **E** and distribution parameters. This is the case for the Bingham distribution (see Bingham 1964 or Mardia 1972, pp. 254–256) and for the March distribution where Cobbold & Gapais (1979) have shown that:

$$E_1 = \frac{\lambda_1}{N}\sum_{i=1}^{N} \frac{l_i^2}{l_i^2\lambda_1 + m_i^2\lambda_2 + n_i^2\lambda_3} \text{ etc.} \quad (9)$$

For such distributions the eigenvalues then specify a specific shape.

NUMERICAL EVALUATION OF EIGENVALUES OF E FOR MARCH DISTRIBUTION

The relationship between eigenvalues of **E** and the principal quadratic elongations which characterise the March distribution is indicated in equation (9). We wish to obtain estimates of λ_1, λ_2 and λ_3 from the eigenvalues E_1, E_2 and E_3, determined from actual data. A direct solution has not been found, instead we evaluate the relationship by a simple numerical simulation.

A uniform square grid was placed at random over an equal-area stereogram. 159 points were obtained at all grid intersections lying within the stereonet and lines corresponding to these intersections determined (Fig. 1). Unit vectors parallel to these lines were used to form the orientation tensor, **E**, and its eigenvalues and eigenvectors determined. These calculations were performed using a digital computer. For the initial distribution, $E_1 = E_2 = E_3$ to within 0.5%, thus the sample conformed closely to that from a uniform distribution. The initial distribution was then deformed by various irrotational strains, and the eigenvalues and eigenvectors of **E** calculated for the resulting distributions. The use of irrotational strain in the simulation was for computational convenience and the results obtained apply to any strain; see argument leading to equation (5). The strain ratios used as input were chosen to give a grid of strain ratios suitable for plotting on a logarithmic plot of E_1/E_2 against E_2/E_3 (Fig. 2). Thus eigenvalues determined from data may be plotted

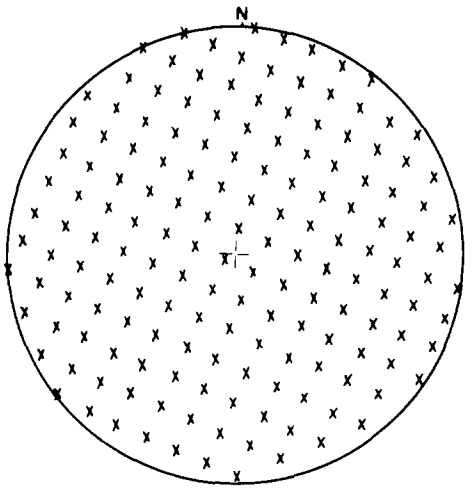

Fig. 1. Sample of 159 lines from uniform distribution used in numerical evaluation of eigenvalues for March distribution. Equal-area stereogram.

on Fig. 2 and their corresponding strain ratios read from the diagram. A more precise strain estimate may be obtained by further simulation using strain values close to that of the initial estimate. In deriving Fig. 2 various initial samples (with $n \simeq 159$) were obtained from the uniform distribution by repositioning the grid on the stereogram. The eigenvalues were fairly insensitive to the initial data if sampled in this way. Random sampling, however, produces a much greater variability. Our objective was not a 'Monte Carlo' simulation to evaluate confidence limits of the strain estimates, but merely a numerical evaluation of the relationship between these and the eigenvalues of **E**.

The graph (Fig. 2) may be used for poles to planes if a and b are interchanged, thus, in Fig. 2 $a = Y/Z$ and $b = X/Y$ for planes. A more detailed and larger version of Fig. 2 is available from the authors.

Cobbold & Gapais (1979) outline an alternative method of numerical evaluation of the relationship between eigenvalues of **E** and strain ratios based on the calculation of angular densities in 576 elemental cones sampled from the March distribution. This method involves significantly greater computation. The simplicity of our technique allows rapid calculation of many simulated strains and sufficient accuracy is obtained for the results to be used in the analysis of most fabric diagrams.

Figure 2 also illustrates some important differences between strain plots and eigenvalue plots. Plane strain ($a = b$ or $K = 1$) does not produce eigenvalues with $E_1/E_2 = E_2/E_3$, as suggested by Woodcock (1977), a feature also noted by Cobbold and Gapais (1979). Woodcock (1977, p. 1235) states that "shape changes plot as straight lines for coaxial homogeneous strains". This is not generally true for either the 3-axis diagram (Owen 1973), to which Woodcock was specifically referring, or the orthogonal logarithmic plot (Fig. 2). Thus the charting of fabric changes during coaxial deformation is more complex than Woodcock suggests.

A final point concerning the use of Fig. 2 should be emphasised. Sampling of a March distribution, even when one is certain the distribution holds, is subject to random variation, possibly approximated by a Fisher distribution (cf. Gaussian treatment of random errors of scalars). Much further work is necessary to establish confidence limits for strain estimates obtained from Fig. 2. Some progress on the testing of axial data has been made using the Bingham distribution (Bingham 1964, Mardia 1972, p. 275). Whilst the Bingham distribution is not identical to the March distribution it has some similarity in form and results obtained for it may be applied approximately to March distributions. The problem of testing Bingham distributions is beyond the scope of this paper and the reader is referred to Mardia (1972) for details.

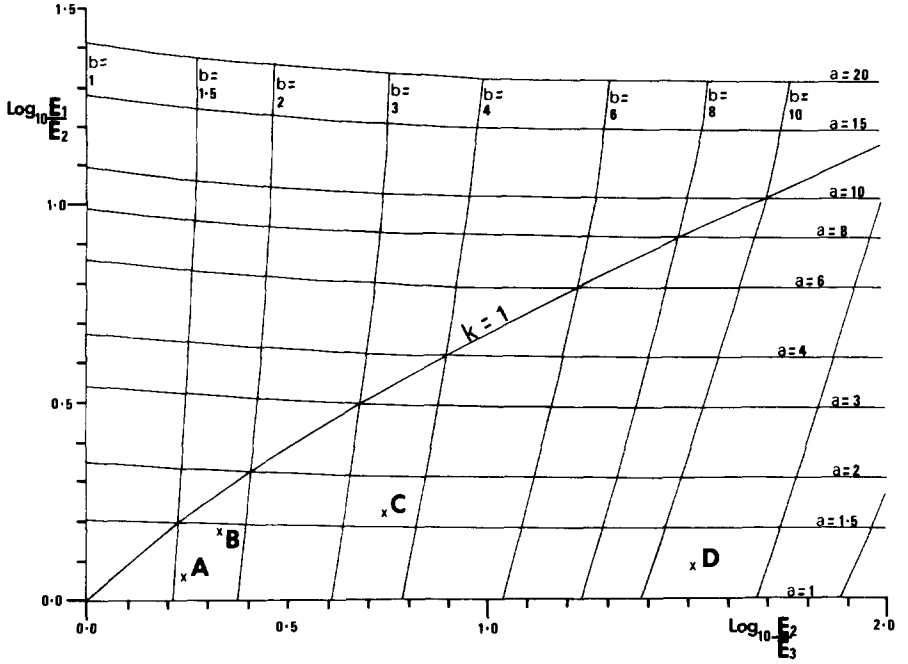

Fig. 2. Eigenvalue ratio plot E_1/E_2 against E_2/E_3 showing values obtained for different strain ratios (a and b). Results for sample localities A, B, C, and D from the Ardara aureole (see Fig. 3) are also plotted.

APPLICATION OF THE METHOD TO FIELD DATA: ANDALUSITES FROM A GRANITE AUREOLE

Andalusite crystals up to 10 cm long occur in the thermal aureole of the Ardara granite, Co Donegal, Ireland. The granite and its aureole have been described by Akaad (1956) and Pitcher & Berger (1972). These authors conclude that the pluton was intruded as a diapir which expanded by injection of granite into its centre. This expansion produced a strong foliation in the outer margins of the pluton. Microstructural evidence shows that the thermal andalusites overprinted the regional schistosity (S_R) which was then flattened around them. This flattening and the bending down of S_R into concordance with the granite contact is considered to be due to the outward radial expansion of the growing pluton.

The andalusites in the aureole develop a pronounced, steep planar fabric towards the contact. This fabric is interpreted as a consequence of the rotation of crystals during the deformation of the envelope of the expanding pluton. The andalusites invariably have a length : breadth ratio of greater than 5 and can therefore be assumed to rotate passively during deformation (Ghosh & Ramberg 1976).

The orientations of the long axes of andalusite crystals were measured from three localities near Clooney in the northern aureole of the granite (Fig. 3). Measurements were made in homogeneous unbanded semipelite containing the regional schistosity. The long axes of the andalusites were plotted on equal-area stereograms. The data form random orientations or planar girdles generally with axial symmetry. The orientation tensor **E** for each sample was calculated and its eigenvalues and eigenvectors found. The eigenvalue ratios were plotted on the orthogonal logarithmic graph (Fig. 2) and the corresponding strain ratios determined. Table 1 summarises the data for the four samples.

From Table 1 and Fig. 4 it can be seen that the degree of preferred orientation and hence the inferred strain ratios vary considerably. A test of uniformity (Mardia 1972, p. 276) was carried out on each sample. Sample A has a random orientation of andalusite long axes, whilst the others are non-random and tests of rotational symmetry (Mardia 1972, p. 277) show these form girdle distributions. Thus the three non-random samples have corresponding strain ratios which plot in the flattening field $K < 1$ (Table 1). S_R dips towards the granite contact and steepens as the strain increases towards the pluton (Table 1). In a general sense the dip of S_R acts as a strain marker and the progressive steepening has been mapped around the pluton (Fig. 3).

Mimetic growth of andalusite parallel to the original schistosity or bedding could produce a non-uniform initial distribution. If this mimetic growth was syn- or post-tectonic then the degree of preferred orientation may

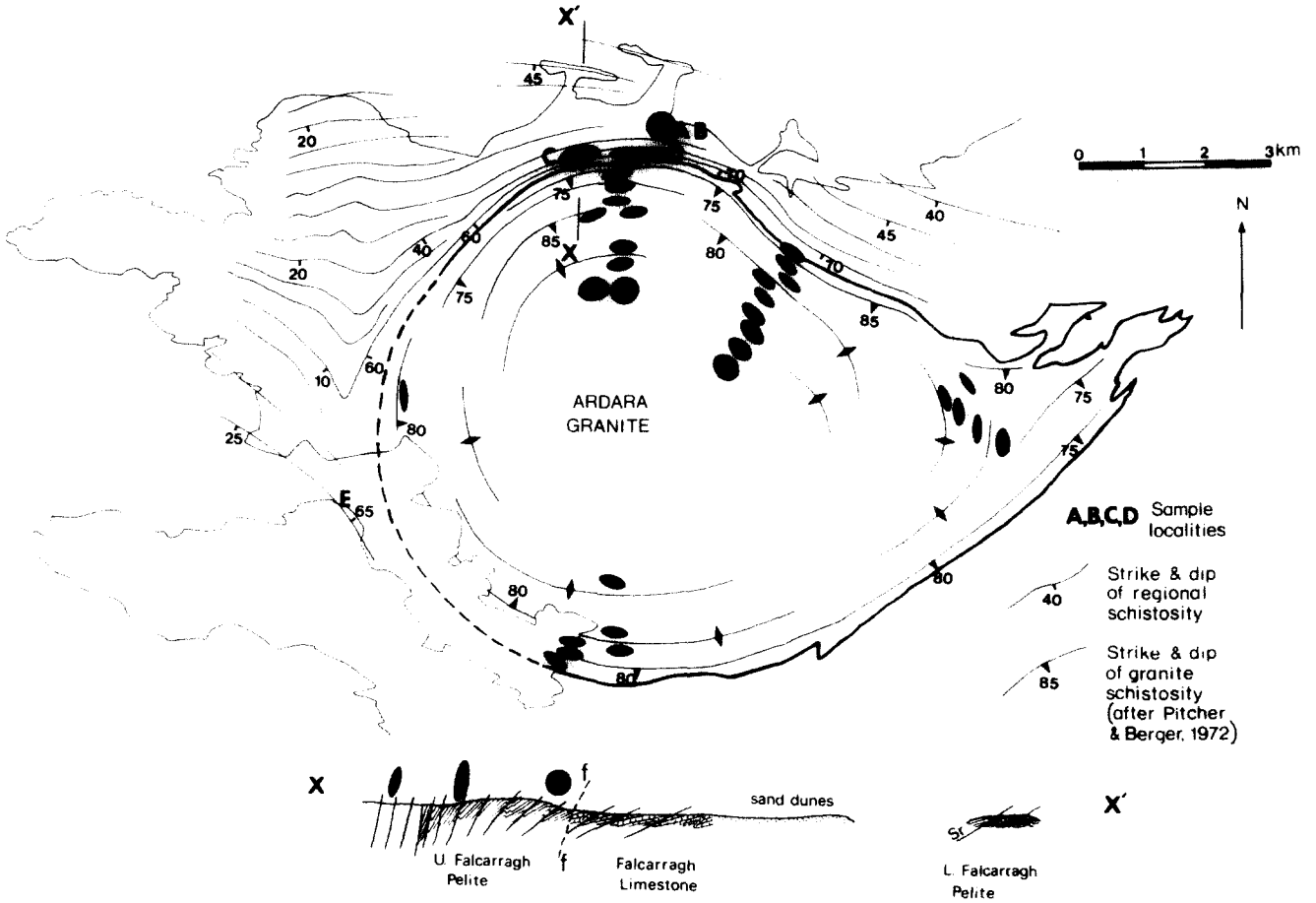

Fig. 3. The Ardara granite and a schematic section through its aureole. Ellipses record the strain related to the intrusion of the pluton. Ellipses within the granite are after Holder (1979).

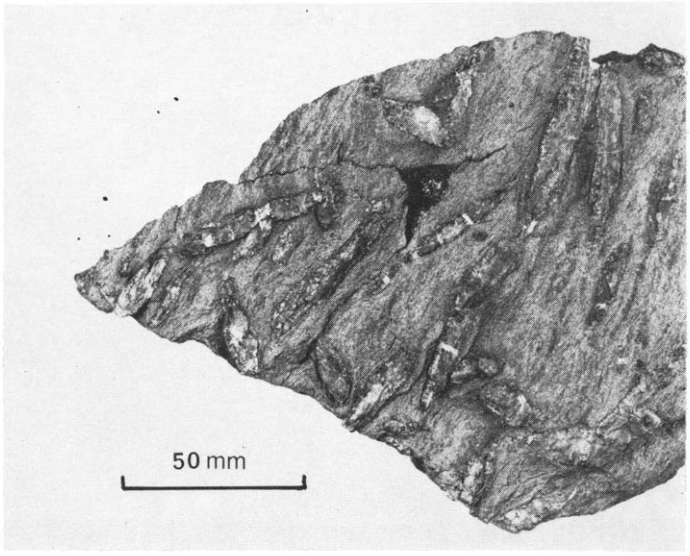

Fig. 5. Boudinaged andalusite crystals from locality E (see Fig. 3).

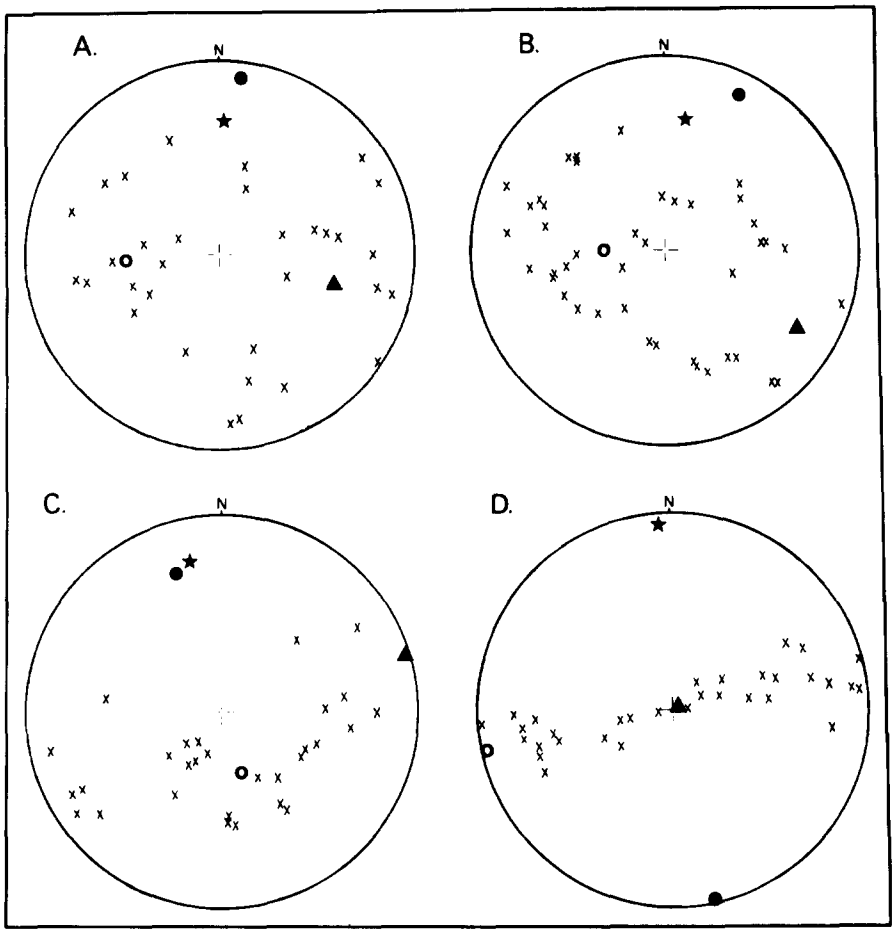

Fig. 4. Equal area stereograms of andalusite long axes, ○, ● and ▲ represent the maximum, minimum and intermediate eigenvalues respectively. is the pole to S_R. Samples A, B, C, and D, the locations of which are shown in Fig. 3.

be expected to increase with the intensification of S_R towards the contact. However, in sample A the andalusites grew across a strong pre-existing regional schistosity producing a random orientation with no mimetic fabric. Elsewhere in the aureole small-scale compositional banding appears to produce a mimetic preferred orientation parallel to bedding, but where bands of homogeneous pelite of greater than 100 mm thick occur, growth is random, as in sample A.

Holder (1979) describes two distinct coaxial deformations in the aureole attributable to granite intrusion, each preceded by a period of andalusite growth. Growth during the later period would have been syntaxial on early formed and rotated crystals so that the final long axis orientations represent the rotations produced by the total strain. This would also hold for a continuous progressive deformation with successive increments of andalusite growing syntaxially on the rotating crystals.

TWO-DIMENSIONAL ANALYSIS OF BOUDINAGED ANDALUSITES

Good evidence for deformation of andalusites comes from Pollaleahy (locality E, Fig. 3) in the southwest of the aureole. Here, approx. 450 m from the contact, crystals lie subparallel to schistosity and bedding, which dip at 68° towards the contact. The high degree of preferred orientation is thought to be due to the strong sedimentary banding parallel to which the andalusites grew mimetically. The crystals were boudinaged during brittle deformation, with no necking between the boudins which are

Table 1. Field data eigenvalue ratios and strain estimates for four samples of andalusite fabrics from the Ardara granite aureole

Sample	No. of andalusites measured	Distance from pluton (metres)	Dip of S_R towards pluton	E_1/E_2	E_2/E_3	X/Y	Y/Z	K
A	32	500	63°	1.14	1.73	1.1	1.5	0.2
B	42	500	63°	1.50	2.16	1.45	1.7	0.64
C	29	150	71°	1.66	5.58	1.6	3.5	0.24
D	32	150	85°	1.19	32.71	1.2	11.5	0.02

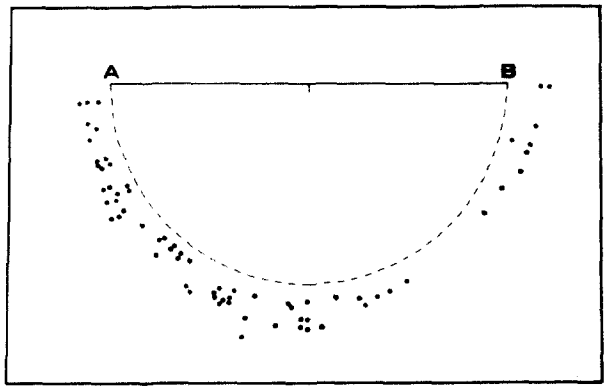

Fig. 6. Pitch and extension of 67 boudinaged andalusites, from locality E (Fig. 3), on schistosity (parallel to bedding). A–B is strike of schistosity.

separated by quartz fibres parallel to the crystal length (Fig. 5).

The pitch and extension of 67 andalusites were measured (Fig. 6) and a best fit ellipse to the data found using the least squares method of Hext (1963). The resulting ellipse has $X = 1.1486$, $Y = 1.1254$, that is a ratio of 1.02 which is not significantly different from unity at 95% level of confidence. Thus the increment of the strain ellipsoid calculated from brittle deformation is oblate ($K \simeq 0$) with $Z < Y \simeq X \simeq 1.137$.

The strain calculated from the extension of the andalusites is a minimum estimate but it supports a flattening deformation in the aureole as deduced from the 3-D andalusite fabrics.

DISCUSSION: IMPLICATIONS OF STRAIN RESULTS TO THE GRANITE INTRUSION MODEL

Pitcher & Berger (1972) suggest that the granite intruded as a diapir which then increased in size by radial extension as an 'expanding balloon'. Equal extension in all directions parallel to the surface of the inflating pluton would produce pure flattening strain. The strain results in this paper, from both the 2-D and 3-D analyses, support flattening parallel to the granite contact as predicted by this model. The 3-D analysis also shows that the strain increases towards the contact.

Holder (1979) has developed the 'expanding balloon' model using oblate strains ($K = 0$) measured from xenoliths in the granite. The unfoliated centre of the pluton has undeformed xenoliths with the strain increasing with increasing foliation towards the margins, the highest strains having X/Z ratios $\simeq 5$. Our results show that the highest strain recorded by the andalusites in the aureole have $X/Z \geq 11$.

Holder has shown how expansion of a pluton with initial radius of about 2.5 km to its present radius of 4–5 km will produce the observed strain in the xenoliths with $X/Z \simeq 5$. The initial diapir may also produce deformation of the aureole which will not be recorded by the xenoliths. The higher strain on the aureole side of the contact could thus reflect the combined strains during the development of the initial diapir and its subsequent expansion.

REFERENCES

Akaad, M. K. 1956. The Ardara granitic diapir of County Donegal, Ireland. *Q. Jl geol. Soc. Lond.* **112,** 263–288.

Bingham, M. S. 1964. Distributions on the sphere and on the projective plane. Unpublished Ph.D. thesis, Yale University.

Cobbold, P. R. & Gapais, D. 1979. Specification of fabric shapes using an eigenvalue method. *Bull. geol. Soc. Am.* **90,** 310–312.

Fara, H. D. & Scheidegger, A. E. 1963. An eigenvalue method for the statistical evaluation of fault plane solutions of earthquakes. *Bull. seism. Soc. Am.* **53,** 811–816.

Ghosh, S. K. & Ramberg, H. 1976. Reorientation of inclusions by combination of pure shear and simple shear. *Tectonophysics* **34,** 1–70.

Harvey, P. K. & Laxton, R. R. 1980. *Tectonophysics* **70,** 285–307.

Hext, G. R. 1963. The estimation of second-order tensors, with related tests and designs. *Biometrika* **50,** 353–373.

Holder, M. T. 1979. An emplacement mechanism for post-tectonic granite and its implications for their geochemical features. In: *Origin of Granite Batholiths: Geochemical Evidence* (edited by Atherton, M. P. & Tarney, J.). Shiva, Kent, 116–128.

Malvern, L. E. 1969. *Introduction to the Mechanics of a Continuous Medium.* Prentice Hall, Englewood Cliffs, N.J.

March, A. 1932. Mathematische Theorie der Regelung nach der Korngestalt bei affiner Deformation. *Z. Kristallogr.* **81,** 285–297.

Mardia, K. V. 1972. *Statistics of Directional Data.* Academic Press, London.

Oertel, G. 1970. Deformation of a slaty, lapillar tuff in the Lake District, England. *Bull. geol. Soc. Am.* **78,** 1173–1187.

Owens, W. H. 1973. Strain modifications of angular density distributions. *Tectonophysics* **16,** 249–261.

Pitcher, W. S. & Berger, A. R. 1972. *The Geology of Donegal: A Study of Granite Emplacement and Unroofing.* Wiley, New York.

Ramsay, J. G. 1967. *Folding and Fracturing of Rocks.* McGraw-Hill, New York.

Ramsden, J. & Cruden, D. M. 1979. Estimating densities in contoured orientation diagrams. *Bull. geol. Soc. Am.* **90,** 229–231.

Sanderson, D. J. 1977. The analysis of finite strain using lines with an initial random orientation. *Tectonophysics* **43,** 199–211.

Scheidegger, A. E. 1964. The tectonic stress and tectonic motion direction in Europe and western Asia as calculated from earthquake fault plane solutions. *Bull. seism. Soc. Am.* **54,** 1519–1528.

Watson, G. S. 1965. Equatorial distributions on a sphere. *Biometrika* **52,** 193–203.

Woodcock, N. H. 1977. Specification of fabric shapes using an eigenvalue method. *Bull. geol. Soc. Am.* **88,** 1231–1236.

Note added in proof

An alternative formulation of the relationship shown in Fig. 2 is given by Harvey & Laxton (1980). The estimation of finite strain from the orientation distribution of passively deformed linear markers: eigenvalue relationships.